

The gravitomagnetic clock effect and its possible observation

H. Lichtenegger^{1*}, L. Iorio², and B. Mashhoon³

¹ Institut für Weltraumforschung, Österreichische Akademie der Wissenschaften, A-8042 Graz, Austria

² Viale Unità di Italia 68, 70125, Bari, Italy

³ Department of Physics and Astronomy, University of Missouri-Columbia, Columbia, Missouri 65211, USA

Key words Gravitomagnetism, gravitomagnetic clock effect, spaceborne clocks.

PACS 04.20.Cv, 04.80.-y

The general relativistic gravitomagnetic clock effect involves a coupling between the orbital motion of a test particle and the rotation of the central mass and results in a difference in the proper periods of two counter-revolving satellites. It is shown that at $\mathcal{O}(c^{-2})$ this effect has a simple analogue in the electromagnetic case. Moreover, in view of a possible measurement of the clock effect in the gravitational field of the Earth, we investigate the influence of some classical perturbing forces of the terrestrial space environment on the orbital motion of test bodies along opposite trajectories.

1 Introduction

According to Einstein's relativistic theory of gravitation, the rotation of a mass induces a particular temporal structure in its surroundings that is clearly revealed by the gravitomagnetic clock effect [1–4]. The purpose of this paper is to discuss this basic effect and emphasize its close correspondence with an analogous electromagnetic phenomenon, thereby extending our previous work on an alternative derivation of the gravitomagnetic clock effect [5]. Moreover, we discuss the prospects for the observation of this interesting effect.

Gravitomagnetism is expected to be ubiquitous, yet its detection is a very difficult venture. Concerning the terrestrial space environment, the GP-B mission [6], aimed at the detection of the gravitomagnetic precessions of the spins [7] of four gyros carried aboard the spacecraft, has been successfully launched in April 2004 and the results are expected to be announced sometime in 2007 [8]; the anticipated accuracy is 1% or better. A test of another gravitomagnetic effect involving the Lense-Thirring precessions [9–10] of the orbits of the LAGEOS and LAGEOS II Earth satellites has been carried out recently [11–12]. The claimed accuracy is 5% at one sigma; for a critical discussion of such a test see [13]. The values of the Lense-Thirring precessions of the inner planets of the Solar System have recently been found to be in general agreement [14] with the latest determinations of the planetary perihelia advances [15], although the errors are still large. However, they might be measured with a better accuracy in the near future when more data will be gathered and processed.

Among the various gravitomagnetic manifestations which might become observable in the solar system within the next few years, the gravitomagnetic clock effect, which involves, among other things, the difference of the sidereal periods of two free counter-orbiting particles about a rotating massive body, is of special interest since it contradicts the common notion of the “dragging of inertial frames”. In the following we will show that this effect has a simple correspondence in the electromagnetic case by considering the motion of a test charge in a dipolar magnetic field, thereby making the nature of the clock effect more

* Corresponding author E-mail: herbert.lichtenegger@oeaw.ac.at, Phone: +43 316 4120 554, Fax: +43 316 4120 590

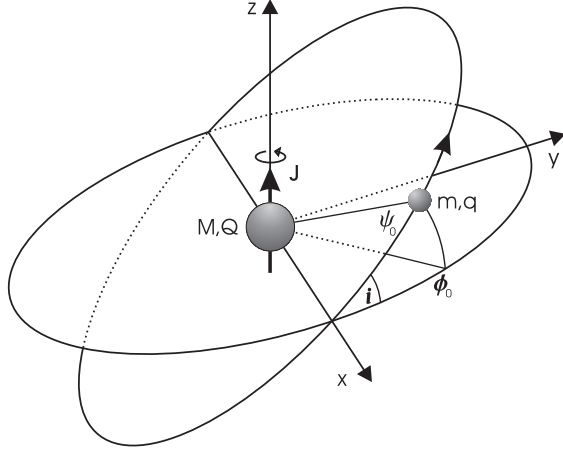


Fig. 1 A test charge (m, q) moves about a central slowly rotating body (M, Q). The figure depicts the initial configuration when the rotation of the source is “turned on”. The unperturbed orbit of the test mass is assumed to be circular; moreover, ψ_0 is the initial angle in the orbital plane, while ϕ_0 is the corresponding angle measured along the equatorial plane to which the orbital plane is tilted by the inclination angle i .

transparent (see also [5]). Finally, the paper ends with a brief discussion of the required accuracy in the determination of the orbital elements in order to test the clock effect in a possible experiment with two counter-revolving satellites about the Earth.

2 The electromagnetic scenario

We consider a spherical body of homogeneously distributed mass M with a charge Q , which rotates with a small angular velocity ω_Q , thereby producing a weak magnetic dipole moment μ_Q . The axis of rotation and the direction of μ_Q shall coincide with the positive z -axis of the background inertial coordinate system. We study the slow motion of a test charge of mass $m \ll M$ and charge q ($qQ < 0$) about the central body such that in the absence of the perturbation due to μ_Q , the motion takes place along a circular inclined orbit, where the nodal line coincides with the x -axis, as shown in Fig. 1. Once the magnetic perturbation is “turned on”, the orbit will no longer be planar; however, the orbital radius can remain constant to first order in the perturbation [5]. Throughout this paper it will be assumed that the test particle moves along a *spherical* orbit of constant radius and that the magnetic field is weak so that second-order effects may be neglected. Moreover, we will ignore all radiative and special relativistic effects on the motion of the electric charges.

In the following we show that the motion of the test mass is modified due to the weak dipolar magnetic field in two ways: (a) the orbital plane precesses about the spin axis of the central body, and (b) the along-track velocity of the test particle is changed.

2.1 The equations of motion

The rigid rotation of the central charge produces a current density \mathbf{j} which involves a magnetic dipole moment

$$\mu_Q = \frac{1}{2c} \int \mathbf{r} \times \mathbf{j} d^3r \quad (1)$$

and hence via the magnetic vector potential

$$\mathbf{A} = \frac{\boldsymbol{\mu}_Q \times \mathbf{r}}{r^3}, \quad (2)$$

the magnetic dipole field

$$\mathbf{B} = \nabla \times \mathbf{A} = \frac{3\mathbf{r}(\mathbf{r} \cdot \boldsymbol{\mu}_Q) - \boldsymbol{\mu}_Q r^2}{r^5}. \quad (3)$$

The motion of the test mass in the electric and magnetic field produced by the central charge is governed by the Lorentz force,

$$\mathbf{F} = q \left(\mathbf{E} + \frac{1}{c} \dot{\mathbf{r}} \times \mathbf{B} \right), \quad (4)$$

where \mathbf{r} is the position vector joining Q with q , an overdot denotes differentiation with respect to time, $\mathbf{E} = (Q/r^3)\mathbf{r}$ is the electric field and \mathbf{B} is given by (3). For later purposes, we formally introduce electric and magnetic charges Q_E, q_E and Q_B, q_B , respectively, and write the equations of motion as

$$\ddot{\mathbf{r}} = \frac{Q_E q_E}{m} \frac{\mathbf{r}}{r^3} + \frac{q_B}{mc} \dot{\mathbf{r}} \times \mathbf{B}, \quad (5)$$

with $Q = Q_E = Q_B$ and $q = q_E = q_B$. It must be emphasized that the magnetic charge (such as Q_B or q_B) introduced here has no connection with the magnetic monopole strength that is assumed to be zero in this work.

2.2 Precession of the orbital plane

Since the orbiting test charge possesses a dipole moment

$$\boldsymbol{\mu}_q = \frac{q_B}{2mc} \boldsymbol{\ell}, \quad (6)$$

where $\boldsymbol{\ell}$ is the orbital angular momentum, a torque $\mathbf{M} = \boldsymbol{\mu}_q \times \mathbf{B}$ will act upon $\boldsymbol{\mu}_q$, leading to a precession of the orbital plane about the z -axis with angular velocity $\boldsymbol{\Omega}_q$ according to $\dot{\boldsymbol{\ell}} = \boldsymbol{\Omega}_q \times \boldsymbol{\ell}$.

In order to find $\boldsymbol{\Omega}_q$, we first determine the vector potential \mathbf{A} . Since the magnetic field \mathbf{B} is associated with the uniform rotation of the central charge of angular momentum $\mathbf{J} = I\boldsymbol{\omega}_Q$, where I is the moment of inertia of M , the dipole moment of the central spherical object becomes

$$\boldsymbol{\mu}_Q = \frac{Q_B}{2Mc} \mathbf{J} = \frac{Q_B I}{2Mc} \boldsymbol{\omega}_Q, \quad (7)$$

or, upon inserting into (2)

$$\mathbf{A} = \alpha \boldsymbol{\omega}_Q \times \mathbf{r}, \quad (8)$$

with $\alpha = Q_B I / (2Mc r^3)$. Vector multiplication of (5) with $m\mathbf{r}$ and using $\mathbf{B} = \alpha \nabla \times (\boldsymbol{\omega}_Q \times \mathbf{r})$ as well as substituting $\mathbf{p} = m\dot{\mathbf{r}}$ in the canonical momentum $\mathbf{P} = \mathbf{p} + (q_B/c)\mathbf{A}$ yield

$$\dot{\mathbf{L}} - \frac{q_B}{c} \left(\dot{\mathbf{r}} \times \mathbf{A} + \mathbf{r} \times \dot{\mathbf{A}} \right) = \frac{2q_B \alpha}{c} \mathbf{r} \times (\dot{\mathbf{r}} \times \boldsymbol{\omega}_Q), \quad (9)$$

where $\mathbf{L} = \mathbf{r} \times \mathbf{P}$. Finally, since $\boldsymbol{\omega}_Q$ and r do not depend upon time, we arrive at

$$\dot{\mathbf{L}} = -\frac{q_B \alpha}{c} \boldsymbol{\omega}_Q \times (\mathbf{r} \times \dot{\mathbf{r}}) = \boldsymbol{\Omega}_q \times \mathbf{L} + \frac{Q_B q_B^2}{2Mmc^3 r^3} \mathbf{J} \times (\mathbf{r} \times \mathbf{A}), \quad (10)$$

where

$$\boldsymbol{\Omega}_q = -\frac{q_B \alpha}{mc} \boldsymbol{\omega}_Q = -\frac{Q_B q_B}{Mm} \frac{\mathbf{J}}{2c^2 r^3}. \quad (11)$$

The last term in equation (10) is of $\mathcal{O}(c^{-4})$, since $\mathbf{A} = \mathcal{O}(c^{-1})$, and is second order in the magnetic perturbation; therefore, it is negligible in accordance with our approximation scheme. It follows that the canonical angular momentum precesses with frequency $\boldsymbol{\Omega}_q$ that is “slow” in comparison with the “fast” orbital motion.

We note that the product $Q_B q_B$ will always be negative, since we are considering attractive forces only, therefore $\boldsymbol{\Omega}_q$ and \mathbf{J} point in the same direction. It is interesting to note that in our approximation scheme, the orbital speed as well as the magnitude of the orbital angular momentum remains constant in accordance with equation (5). What we have demonstrated here for canonical angular momentum also holds true, when averaged with respect to the “fast” orbital motion, for $\boldsymbol{\ell} = \mathbf{r} \times \mathbf{p}$. That is, it can be shown that on the average, the orbital plane of the test charge is “dragged” in the same sense as the rotation of the central charge.

2.3 The change in the orbital velocity

In the following we will calculate the change in the along-track velocity due to the magnetic dipole field (3). The result can be understood heuristically by determining the magnetic flux through the orbital plane. If we assume that the magnetic field is switched on and increases from zero to \mathbf{B} , then by means of Faraday’s law we can calculate the electric field strength E induced in the orbital plane due to the varying magnetic field and obtain

$$E = \frac{1}{2cr^2} \frac{d\mu_Q}{dt} \cos i, \quad (12)$$

where i is the inclination angle. From (12) and $q_B E = m dv/dt = m r d\dot{\psi}/dt$, the change in the angular velocity $\Delta\dot{\psi}$ caused by the dipolar magnetic field becomes

$$\Delta\dot{\psi} = \frac{Q_B q_B}{Mm} \frac{J}{4c^2 r^3} \cos i; \quad (13)$$

this result can be obtained directly starting from equation (5). Since $Q_B q_B < 0$, we see that the test charge moves slower in the prograde direction (i.e. in the direction of the rotation of the source), and faster in the retrograde direction as compared to a situation without the magnetic field. This behavior is also intuitively confirmed by the subsequent evolution of the motion under the action of the Lorentz force: for the prograde motion the Lorentz force points away from the source and weakens the attractive Coulomb force. We note that this feature is independent of the sign of the revolving charge, because the exchange of the signs of the central and orbiting charge will also change the direction of the magnetic field.

The change in the velocity of the revolving charge can also be anticipated by virtue of Lenz’s rule: the induced current will have such a direction as to counteract its own source. Indeed, let us replace the rotating source by a single current loop and the orbit of the revolving charge by a conducting wire concentric to the inner loop. Any change ΔI of the inner current will induce a current in the outer wire having the same direction as ΔI , thus leading to an increase of the magnetic flux through the inner loop. This additional flux in turn induces a current opposite to ΔI and thus opposes a change of the inner current.

2.4 Time of revolution

According to (13), the velocity of the test charge depends on the direction of the motion and thus its period will be different for pro- and retrograde orbits. If the magnetic field is absent, the Kepler period

is $T_{\kappa} = 2\pi/\dot{\psi}_{\kappa}$, with the frequency $\dot{\psi}_{\kappa} = (|Q_{\text{E}}q_{\text{E}}|/mr^3)^{1/2}$, while in the presence of a magnetic field, $\dot{\psi} = \dot{\psi}_{\kappa} + \Delta\dot{\psi}$ and the time of revolution T^* becomes

$$T^* = \frac{2\pi}{\dot{\psi}} \simeq \frac{2\pi}{\dot{\psi}_{\kappa}} \left(1 - \frac{\Delta\dot{\psi}}{\dot{\psi}_{\kappa}} \right) = \frac{2\pi}{\dot{\psi}_{\kappa}} \left(1 - \frac{1}{\dot{\psi}_{\kappa}} \frac{q_{\text{B}}\mu_{\text{Q}}}{2mcr^3} \cos i \right). \quad (14)$$

The difference in the period for two orbits with different inclinations i_1 and i_2 is immediately found from (14) and (7) to be

$$T_1^* - T_2^* = \frac{1}{2} \pi \frac{J}{Mc^2} (\cos i_1 - \cos i_2) \quad (15)$$

for electric charges. Note that this time difference, which refers to the closure of the angle ψ in the orbital plane, depends only on the specific angular momentum of the source, but neither on the charge nor the distance r of the test mass, and it is maximum for opposite equatorial orbits (i.e. $i_1 = 0$, $i_2 = \pi$ or vice versa).

2.5 The magnetic clock effect

As demonstrated in the preceding paragraphs, the motion of a test charge in a central Coulomb field together with a weak dipolar magnetic field results in a slow precession of the orbital plane as well as a slightly increased or decreased along-track velocity.

An inertial observer will define the period of the particle as the time elapsed between two successive crossings of a fixed plane in space, and consequently this period will differ from (14) due to the nodal precession of the orbital plane. The time of revolution as measured by the inertial observer can be calculated by noting that the particle's position angle ψ in the orbital plane is related to the corresponding angle ϕ measured from the lines of the ascending nodes in the equatorial plane by

$$\tan \phi = \tan \psi \cos i. \quad (16)$$

Now, let $\psi_0 = \psi(t=0)$ and $\phi_0 = \phi(t=0)$ denote the initial position of the particle and T be its period with respect to the inertial frame, where $T = T^* + \Delta T$ and $\Delta T \ll T, T^*$. The angle swept over by the particle after completion of one revolution as seen by the inertial observer in the orbital plane becomes $\psi_0 + \dot{\psi}T - \omega_{\text{q}}T \cos i$, while in the equatorial plane this corresponds to $\phi_0 + 2\pi - \omega_{\text{q}}T$ and therefore

$$\tan(\phi_0 - \omega_{\text{q}}T) = \tan(\psi_0 + \dot{\psi}T - \omega_{\text{q}}T \cos i) \cos i. \quad (17)$$

By means of trigonometric relations and by noting that $\tan \dot{\psi}T \simeq \dot{\psi}\Delta T$, $\tan \omega_{\text{q}}T \simeq \omega_{\text{q}}T^*$ and $\dot{\psi}^{-1} \simeq \dot{\psi}_{\kappa}^{-1}(1 - \Delta\dot{\psi}/\dot{\psi}_{\kappa})$ together with (11) and (13), we finally obtain to first order by virtue of (16)

$$T = \frac{2\pi}{\dot{\psi}_{\kappa}} \left[1 - \frac{1}{\dot{\psi}_{\kappa}} \frac{\mu_{\text{Q}}q_{\text{B}}}{2mcr^3} (1 - 2 \tan^2 i \cos^2 \psi_0) \cos i \right]. \quad (18)$$

From this equation, the difference in the periods for two orbits with inclination i_1 and i_2 is found to be

$$T_1 - T_2 = \frac{\pi q_{\text{B}}}{|Q_{\text{E}}q_{\text{E}}|} \frac{\mu_{\text{Q}}}{c} [2 \cos^2 \psi_0 (\tan^2 i_1 \cos i_1 - \tan^2 i_2 \cos i_2) - \cos i_1 + \cos i_2], \quad (19)$$

which reduces for $q_{\text{E}} = q_{\text{B}}$ and $Q_{\text{E}} = Q_{\text{B}}$ to the magnetic clock effect

$$T_1 - T_2 = -\frac{1}{2} \pi \frac{J}{Mc^2} [2 \cos^2 \psi_0 (\tan^2 i_1 \cos i_1 - \tan^2 i_2 \cos i_2) - \cos i_1 + \cos i_2]; \quad (20)$$

for opposite or supplementary orbits ($i_1 = i$, $i_2 = \pi - i$), this relation simplifies to

$$T_1 - T_2 = \pi \frac{J}{Mc^2} (1 - 2 \tan^2 i \cos^2 \psi_0) \cos i. \quad (21)$$

It should be emphasized that the dependence of the period (and of the time difference in turn) on ψ_0 is due to the non-linear relation (16).

It is interesting to note that the period for a prograde orbit is longer than the Kepler period for low inclinations (remember that $q_B \mu_Q < 0$) and shorter for high inclinations, because in the first case the lower orbital velocity implies $T > T_K$, while in the latter case the nodal precession, which makes the period to decrease, dominates.

3 The gravitomagnetic scenario

In the case of slow motion and weak gravitational fields, the spacetime metric can be approximated by

$$g_{\mu\nu} = \eta_{\mu\nu} + h_{\mu\nu}, \quad (22)$$

where $\eta_{\mu\nu} = \text{diag}(-1, +1, +1, +1)$ is the Minkowski metric and $|h_{\mu\nu}| \ll 1$ is a small correction so that only terms linear in $h_{\mu\nu}$ will be of significance.

3.1 The equations of motion

As in the electromagnetic case, the mass current density \mathbf{j}_g associated with the rotation of the central mass with angular momentum \mathbf{J} produces a dipole moment

$$\boldsymbol{\mu}_g = \frac{1}{2c} \int \mathbf{r} \times \mathbf{j}_g d^3r \equiv \frac{G}{c} \mathbf{J} \quad (23)$$

with the corresponding vector potential

$$\mathbf{A}_g = \frac{G}{c} \frac{\mathbf{J} \times \mathbf{r}}{r^3}, \quad (24)$$

which implies the gravitomagnetic dipole field

$$\mathbf{B}_g = \nabla \times \mathbf{A}_g = \frac{G}{c} \frac{3\mathbf{r}(\mathbf{r} \cdot \mathbf{J}) - \mathbf{J}r^2}{r^5} \quad (25)$$

analogous to (3).

In the case of weak perturbations (22) and upon restricting to static fields, the geodesic equation can be written in the form [4]

$$\mathbf{F} = -m \left(\mathbf{E}_g + \boldsymbol{\mathcal{E}}_g + \frac{2}{c} \dot{\mathbf{r}} \times \mathbf{B}_g \right), \quad (26)$$

where $\mathbf{E}_g = GM\mathbf{r}/r^3$ and $\boldsymbol{\mathcal{E}}_g = \mathcal{O}(c^{-2})$ is the post-Newtonian gravitoelectric field. As has been first pointed out in [16], a complete correspondence with electromagnetism can be achieved by introducing the notion of gravitoelectric and gravitomagnetic charges, q_E and q_B , respectively, and ignoring $\boldsymbol{\mathcal{E}}_g$. The equation of motion (26) thus becomes

$$\ddot{\mathbf{r}} = \frac{GMq_E}{m} \frac{\mathbf{r}}{r^3} + \frac{q_B}{mc} \dot{\mathbf{r}} \times \mathbf{B}_g, \quad (27)$$

in perfect agreement with (5). The appearance of the factor 2 in the ‘‘magnetic’’ force term of (26) suggests $q_B = -2m$ as well as $q_E = -m$, where the additional minus sign accounts for the fact that gravitational charges of opposite polarity, like in the electromagnetic case, should be attractive. From (27) we also read $Q_E = GM$ and consequently $Q_B = 2GM$.

3.2 The gravitomagnetic clock effect

Because the equations of motion of electrodynamics and linear general relativity are formally equivalent, in the weak-field and low-velocity limit gravitational phenomena are expected to be similar to those known in electrodynamics. Therefore, by means of the substitutions derived in the preceding section,

$$\begin{aligned} q_E &\rightarrow -m, & Q_E &\rightarrow GM, \\ q_B &\rightarrow -2m, & Q_B &\rightarrow 2GM, \end{aligned} \quad (28)$$

we can directly translate electromagnetic phenomena into the corresponding gravitoelectromagnetic phenomena. It is important to note that the ratio of the gravitomagnetic charge to the gravitoelectric charge is always 2, which corresponds to the spin-2 character of linear gravitation. This is in agreement with the fact that the ratio of the magnetic charge to the electric charge is always unity in Maxwell's spin-1 electrodynamics.

With $\mu_Q \rightarrow GJ/c$ from (7) we immediately obtain by virtue of (11)

$$\Omega_{\text{LT}} = \frac{2GJ}{c^2 r^3}, \quad (29)$$

which is the well-known Lense-Thirring precession of the node of the orbital plane of a satellite. Further, let T_{\pm} denote the period of revolution in the same (+) and opposite (-) sense as the rotation of the source, then (18) translates into

$$T_{\pm} = T_k \pm 2\pi \frac{J}{Mc^2} (1 - 2 \tan^2 i \cos^2 \psi_0) \cos i, \quad (30)$$

which is equivalent to equation (35) of [2] if terms of $\mathcal{O}(c^{-4})$ are neglected. Finally, for opposite equatorial orbits it follows from (30) that

$$T_+ - T_- = 4\pi \frac{J}{Mc^2}, \quad (31)$$

yielding the gravitomagnetic clock effect obtained in [1]. It is an interesting fact that (31), as well as its magnetic counterpart (21), neither depends on the coupling constant nor on the distance r of the test masses. The reason for this is seen by inspection of (13) and (14): both the square of the Kepler frequency and the induced velocity change depend on G/r^3 ($Q_B \rightarrow 2GM$ in (13)) and hence it will not appear in the expression $T_+ - T_- \propto \Delta\dot{\psi}/\dot{\psi}_k^2$. This result is a consequence of the r^{-3} fall-off of the dipolar magnetic field. In a homogeneous magnetic field, for instance, $\Delta\dot{\psi}$ will be independent of the distance and the time difference will thus become $T_+ - T_- \propto r^3$. Further, the absence of the gravitational constant G in (31) allows the time difference to become relatively large; inserting the appropriate values for the Earth into (31) yields $T_+ - T_- \sim 10^{-7}$ s.

4 An alternative clock effect

If we introduce the angle $\xi = \omega + \Omega \cos i + \mathcal{M}$, where $\omega, \Omega, \mathcal{M}$ and i are the argument of pericenter, the longitude of the ascending node, the mean anomaly and the orbital inclination, respectively, its temporal rate of change is given by

$$\frac{d\xi}{dt} = \frac{d\omega}{dt} + \frac{d\Omega}{dt} \cos i - \Omega \sin i \frac{di}{dt} + \frac{d\mathcal{M}}{dt}. \quad (32)$$

Upon inserting the secular contributions of the oblateness of the Earth as well as the corresponding Schwarzschild and Lense-Thirring rates we find that the time needed for ξ to cover an angle of 2π is given by

$$T_{\xi} = \frac{2\pi}{\bar{n}} \left[1 + J_2 \frac{3R_E^2 (1 + \sqrt{1 - e^2})}{4a^2(1 - e^2)^2} (1 - 3 \cos^2 i) - \frac{3\bar{n}^2 a^2}{c^2(1 - e^2)} + \frac{4\bar{n}J \cos i}{c^2 M(1 - e^2)^{3/2}} \right], \quad (33)$$

where a , e and \bar{n} are the semimajor axis, eccentricity and mean motion, and R_E , J and M are the radius, angular momentum and mass of the Earth, respectively; J_2 is the lowest zonal harmonic coefficient in the multipolar expansion of the terrestrial gravitational field. For satellites along identical but opposite orbits, all but the last term in (33) cancel when taking the time difference in the periods of ξ , revealing the gravitomagnetic signature

$$T_\xi^+ - T_\xi^- = \frac{16\pi J \cos i}{c^2 M (1 - e^2)^{3/2}}, \quad (34)$$

which could in principle be measured by means of two counter-revolving satellites around the Earth. We note that (34) reduces to equation (14) of [17] in the case of nearly equatorial and circular orbits.

5 Error analysis

Equation (34) holds only for the ideal case that the two orbits are identical and the orbital elements are exactly known. In a real experiment, both the orbits will differ from each other due to injection errors and the elements are only determined with limited accuracy. These residuals will contribute to the difference in equation (34) and must hence be kept less than the Lense-Thirring difference. Although equatorial orbits would be favorable, however, since most satellite laser ranging stations are located in the northern hemisphere, inclined orbits are more suitable from an observational point of view. For a nominal orbit with $a = 12\,000$ km, $e = 0.01$ and $i = 63.4^\circ$, which represents a frozen perigee configuration, the upper panel in Fig. 2 displays the maximum allowable uncertainty of Δa , Δe and Δi , as a function of the corresponding orbital elements, while the lower panel illustrates the maximum allowable change of $\Delta(GM)/GM$ and $\Delta J_2/J_2$ with respect to the deviation from the nominal orbit of $a = 12\,000$ km. As can be seen, a relative accuracy of $\Delta a/a < 6 \times 10^{-12}$, $\Delta e/e < 1 \times 10^{-4}$, $\Delta i/i < 8 \times 10^{-9}$ is required, while the uncertainties in the values of GM and J_2 are of minor importance, since they are known to an accuracy of $\Delta(GM)/GM \sim 10^{-9}$ and $\Delta J_2/J_2 \sim 10^{-7}$ [18]. With about 2500 revolutions per year, after 4 years of observation and for a target error of 1%, the semimajor axis must be known with an accuracy of about 1 part in 10^9 , i.e. to a few cm, e to 1% and i to 0.0001%. The stringent limit for i is due to the high inclination of the nominal orbit; for near equatorial orbits this limit becomes less severe [17]. Finally, we note that care must also be taken in the accurate modelling of all non-gravitational perturbations. In

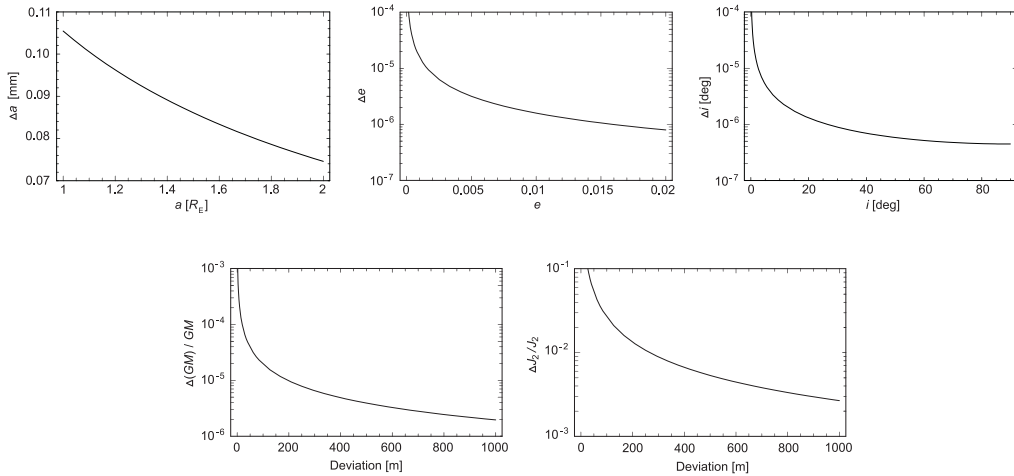


Fig. 2 Maximum tolerable error of various values for a nominal orbit of $a = 12\,000$ km, $e = 0.01$ and $i = 63.4^\circ$.

this case, however, one would greatly benefit from the experience gained in the LAGEOS-LAGEOS II Lense-Thirring experiment.

6 Conclusion

It has been shown that the gravitomagnetic clock effect for spherical orbits has a simple correspondence with the electromagnetic case. The difference in the sidereal periods of two counter-revolving charges about a central spinning charge is due both to the different velocities of the test charges and to the precession of the orbital plane. The slower prograde velocity, which in the gravitational case is against the common notion of the dragging of inertial frames, can be considered as a consequence of the Lenz rule. The gravitomagnetic clock effect is obtained by simply substituting the electric and magnetic charges by the corresponding gravitoelectric and gravitomagnetic ones. With regard to the gravitational perturbations, a key issue for a possible observation of the clock effect with two counter-orbiting satellites is the stringent requirement in the accuracy of the inclinations.

References

- [1] J.M. Cohen and B. Mashhoon, *Phys. Lett. A* **181**, 353–358 (1993).
- [2] B. Mashhoon, F. Gronwald, and D.S. Theiss, *Ann. Physik* **8**, 135–152 (1999).
- [3] B. Mashhoon, F. Gronwald, and H. Lichtenegger, in: *Gyros, Clocks, Interferometers...: Testing Relativistic Gravity in Space*, edited by C. Lämmerzahl, C. W. F. Everitt and F. W. Hehl (Springer, Berlin, 2001), pp. 83-108.
- [4] B. Mashhoon, L. Iorio, and H. Lichtenegger, *Phys. Lett. A* **292**, 49-57 (2001).
- [5] L. Iorio, H. Lichtenegger, and B. Mashhoon, *Class. Quantum Grav.* **19**, 39-49 (2002).
- [6] C.W.F. Everitt et al., in: *Gyros, Clocks, Interferometers...: Testing Relativistic Gravity in Space*, edited by C. Lämmerzahl, C. W. F. Everitt and F. W. Hehl (Springer, Berlin, 2001), pp. 52-82.
- [7] L. Schiff, *Phys. Rev. Lett.* **4**, 215–217 (1960).
- [8] For information about Gravity Probe B, see <http://einstein.stanford.edu>.
- [9] J. Lense and H. Thirring, *Phys. Z.* **19**, 156-163 (1918).
- [10] B. Mashhoon, F. W. Hehl, and D. S. Theiss, *Gen. Rel. Grav.* **16**, 711–750 (1984).
- [11] L. Iorio and A. Morea, *Gen. Rel. Grav.* **36**, 1321–1333 (2004).
- [12] I. Ciufolini and E.C. Pavlis, *Nature* **431**, 958–960 (2004).
- [13] L. Iorio, *J. of Geodesy* **80**, 128–136 (2006).
- [14] L. Iorio, First preliminary evidence of the general relativistic gravitomagnetic field of the Sun and new constraints on a Yukawa-like fifth force, (2005) [<http://arxiv.org/abs/gr-qc/0507041>].
- [15] E.V. Pitjeva, *Astron. Lett.* **31**, 340–349, 2005.
- [16] B. Mashhoon, *Phys. Lett. A* **173**, 347–354 (1993).
- [17] L. Iorio and H.I.M. Lichtenegger, *Class. Quantum Grav.* **22**, 119–132 (2005).
- [18] D.D. McCarthy and G. Petit (eds.), *IERS Conventions (2003)*, IERS Technical Note No. 32 (Verlag des Bundesamts für Kartographie und Geodäsie, Frankfurt am Main, 2004).